Tanzania Journal of Science 47(2): 405-420, 2021
ISSN 0856-1761, e-ISSN 2507-7961

Copper Slag as a Potential Waste Filler for Polyethylene-Based Composites Manufacturing

Aleksander Hejna[1*], Paulina Kosmela[1], Mateusz Barczewski[2], Olga Mysiukiewicz[2] and Adam Piasecki[3]

[1] *Department of Polymer Technology, Gdansk University of Technology, Narutowicza 11/12 80-233 Gdansk, Poland*

[2] *Poznan University of Technology, Faculty of Mechanical Engineering, Institute of Materials Technology, Piotrowo 3, 61-138 Poznan, Poland*

[3] *Poznan University of Technology, Faculty of Materials Engineering and Technical Physics, Institute of Materials Engineering, Piotrowo 3, 61-138 Poznan, Poland*

aleksander.hejna@pg.edu.pl; paulina.kosmela@pg.edu.pl; mateusz.barczewski@put.poznan.pl; olga.mysiukiewicz@put.poznan.pl; adam.piasecki@put.poznan.pl

**Corresponding author e-mail: aleksander.hejna@pg.edu.pl*

Received 2 Mar 2021, Revised 7 Apr 2021, Accepted 21 Apr 2021, Published May 2021

Abstract

The present study aimed to analyze the application of waste material from copper production–copper slag (ŻŻL) as filler for composites based on the high-density polyethylene (HDPE). Copper slag filler was introduced in the amounts of 1–20 wt%, and its influence on the appearance (color analysis), chemical structure (Fourier-transform infrared (FTIR) spectroscopy), microstructure (optical microscopy), as well as static (tensile tests) and dynamic (dynamical mechanical analysis (DMA)) mechanical properties of composites were investigated. Proper dispersion of filler implicated that the incorporation of up to 5 wt% of filler caused only slight, 5% drop of tensile strength, with the simultaneous 16% rise of Young's modulus. Further increase of filler loading resulted in higher values of porosity and the rise of the adhesion factor, determined from DMA results, which led to the deterioration of mechanical performance. Moreover, spectroscopic analysis of PE-ŻŻL composites indicated that the analyzed filler might be applied as a coloring agent, and the appearance of composites may be engineered by adjustment of filler loading.

Keywords: polyethylene, copper slag, mechanical properties, structure, composite, particle reinforced composite.

Introduction

Polyethylene (PE) is currently the most used and processed polymer. The main areas of use of polyethylene are packaging (Czarnecka-Komorowska and Wiszumirska 2020), in particular, the production of cast and blow-molded films. However, it is also widely used in construction, agriculture, the automotive, civil engineering, and electrical industries (He et al. 2012, Kasirajan and Ngouajio 2012, Luo et al. 2015). The value of the polyethylene sales market in 2018 was 103.49 billion USD and is expected to increase to 143.3 in 2026 (Fortune Business Insights 2019). The widespread use of polyethylene results in great possibilities of modifying its macromolecular structure, including controlled molecular weight and its polydispersity (Peterlin 1971). The chemical structure of PE is presented in Figure 1.

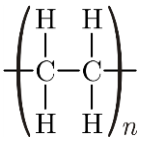

Figure 1: Chemical structure of polyethylene (PE).

While polyethylene is characterized by excellent impact resistance, very low glass transition temperature (T_g), and chemical resistance, its mechanical properties do not allow to define it as an engineering polymer. One way to improve mechanical properties is to apply it as a matrix of polymeric composites. In so far published studies, as well as industrial practice, numerous examples of the use of polyethylene composites reinforced with fibrous- and particle-shaped fillers have been noted (Gnatowski et al. 2018, Kalaprasad et al. 1997, Rudawska et al. 2017). Despite the high chemical resistance and low reactivity, many cases of polyethylene nanocomposite production have been demonstrated. Studies published so far take into account both the production of nanocomposites modified with inorganic fillers such as halloysite nanotubes (Li and Li 2016), various grades of carbon nanotubes (Arora and Pathak 2020, Burzynski et al. 2020), as well as hybrid organic-inorganic fillers with a chemical structure that allows obtaining the highest compatibility and efficiency of polymer matrix interactions (Niemczyk et al. 2016, 2019).

Another approach to the production of polymer composites based on non-biodegradable petrochemical polymers, conducted in order to improve their sustainability, is the application of waste materials as fillers or/and the use of recycled polymer matrix. The use of waste materials from various industries to produce polymer composites has become not only a common trend in the scientific community but also a noticeable phenomenon in the industrial production conditions. Depending on the availability and desired applications, thermoplastic and thermoset polymers are modified with inorganic and organic waste materials used as fillers (Bhagavatheswaran et al. 2019, Członka et al. 2020, Kairytė et al. 2020). While composites reinforced with lignocellulosic fillers, including wood flour or wooden ground parts of plants, are commonly used (Ryszkowska and Sałasińska 2010, Sałasińska and Ryszkowska 2013, Sałasińska et al. 2018), in many cases, the long-term exposure of highly filled systems to environmental conditions limits their use (Gunjal et al. 2020). While the polyethylene matrix is non-biodegradable and hydrophobic, the introduction of high amounts of plant fillers, with the ability for water absorption during long-time exposure to water, may cause significant deterioration of mechanical properties of the composites (Bajwa et al. 2009, Friedrich and Lubile 2016).

The application of inorganic waste fillers is an excellent way to improve the sustainability of polyethylene-based composites without significant deterioration of their environmental resistance. Even though some examples of the applications of inorganic waste fillers such as basalt powder (Barczewski et al. 2019) or recycled carbon fiber (Andrzejewski et al. 2018) for thermoplastic composites can be found in the literature, this subject needs a deeper insight.

Copper slag (ŻŻL) is an oxide-based waste product resulting from copper production in a pyrometallurgical process from ore (Gorai et al. 2003). It typically contains compounds of iron, silicon, aluminum, calcium, and copper (Erdenebold et al. 2018), and its properties resemble those of basalt of obsidian (Gorai et al. 2003). Enormous amounts of copper slag are generated (about 2.2-3.0 tons of copper slag per 1 ton of pure copper) (Erdenebold et al. 2018) and even though this by-product can be utilized for abrasive applications (Mugford et al. 2017) in production of cement and concrete (Al-Jabri et al. 2011, Shi et al. 2008) as well as ceramic tiles (Gorai et al. 2003), its potential is not fully capitalized. Taking into consideration the beneficial properties of copper slag, such as high hardness (6-7 Mohs) (Gorai et al. 2003), abrasion resistance, low moisture absorption

(Shi et al. 2008), thermal resistance and availability at a low price, this waste product can be a good candidate for a sustainable filler for polyethylene. The reviewed literature suggest that copper slag is hardly used in thermoplastic composites. Therefore, this study aimed to evaluate the influence of ŻŻL on morphology, appearance, mechanical performance, and thermal properties of polyethylene-based composites in order to assess the possibilities of its utilization in industrial applications.

Materials and Methods

Materials

The commercial-grade of high-density polyethylene M300054 delivered by SABIC (Bergen op Zoom, The Netherlands), with a density of 0.954 g/cm^3 and melt flow rate (MFR) 30 g/10 min (190 °C, 2.16 kg), was used as a polymeric matrix for the manufacturing of investigated composites. Copper slag was received from the processing of Polish copper-rich deposits, as a by-product generated from the smelting of copper blister in suspension furnace during pyrometallurgical copper production. It was characterized by a density of 3.040 g/cm^3.

Samples Preparation

The composites were prepared in a melt-mixing method. Firstly, in order to equalize the bulk density of the matrix and the filler, polyethylene was pulverized into a fine powder using a Tria 25-16/TC-SL high-speed knife grinder. The obtained powder was mixed with 1, 2, 5, 10, and 20 wt% of the filler. The components were blended with a ZAMAK EH16.2D co-rotating twin-screw extruder operating at 100 rpm, with the maximum temperature of the process being 190 °C. Resulting composites were cooled at air and pelletized. The samples for testing were compression molded at 170 °C and 4.9 MPa for 2 min, then kept under pressure at room temperature for another 5 min to prevent warpage. The unfilled polyethylene was processed in the same way as its composites.

Measurements

The chemical structures of HDPE and its composites were determined using Fourier transform infrared (FTIR) spectroscopy performed by a Nicolet Spectrometer IR200 from Thermo Scientific (USA). The device had ATR attachment with a diamond crystal. Measurements were performed with 1 cm^{-1} resolution in the range from 4000 to 400 cm^{-1} and 64 scans.

Microscopic observations of the filler, as well as polyethylene and its composites, were performed using an optical microscope Opta-Tech SK Series microscope. The obtained pictures were digitally edited and registered using dedicated software–Capture V2.0 Revolutionary computational imaging software (DeltaPix).

The surface composition of the filer was analyzed by energy-dispersive X-ray spectroscopy (EDS) using a Princeton Gamma-Tech unit equipped with a digital prism spectrometer (Princeton Gamma-Tech, Princeton, NJ, USA). Representative parts of each sample (200 × 200 μm^2) were analyzed to determine their actual surface composition.

The density of samples was measured based on the Archimedes method, as described in ISO 1183. Accordingly, all measurements were carried out at room temperature (21 °C) in methanol medium.

To determine the porosity of the prepared composites, theoretical values of their density were calculated according to the simple rule of mixture, expressed by the following equation (1):

$$\rho_c = \rho_m \cdot (1 - \varphi) + \rho_f \varphi \qquad (1)$$

where: ρ_c = density of the composite, g/cm^3; ρ_m = density of the matrix, g/cm^3; ρ_f = density of the filler, g/cm^3; and φ = volume fraction of the filler.

Using obtained values of the density, composite's porosity was calculated (2):

$$p = \frac{\rho_{theo} - \rho_{exp}}{\rho_{theo}} \cdot 100\% \qquad (2)$$

where: p = porosity of the material, %; ρ_{theo} = theoretical value of density, g/cm^3; and ρ_{exp} =

the experimental value of density of composite, g/cm^3.

The tensile strength and elongation at break were estimated following ISO 527 for dumbbell samples type 5B. Tensile tests were performed on a Zwick/Roell Z020 apparatus with a cell load capacity of 20 kN at a constant speed of 5 and 50 mm/min. Standard indicates that with the lowering of the gauge length, the speed of the test should be reduced proportionally. Therefore, we aimed to examine the effect of varying test speed.

The dynamic mechanical analysis was conducted on a DMA Q800 TA Instruments apparatus (TA Instruments, USA). Samples with dimensions of 40 × 10 × 2 mm, prepared by compression molding, were loaded with variable sinusoidal deformation forces in the single cantilever bending mode at the frequency of 1 Hz under the temperature rising rate of 4 °C/min, ranging the temperature from -100 to 100 °C.

The color of polyethylene and its composites was evaluated according to the International Commission on Illumination (CIE) through L*a*b* coordinates (International Commission on Illumination 1978). In this system, L* is the color lightness (L* = 0 for black and L* = 100 for white), a* is the green(-) / red(+) axis, and b* is the blue(-) / yellow(+) axis. The color was determined by optical spectroscopy using HunterLab Miniscan MS/S-4000S spectrophotometer, placed additionally in a specially designed light trap chamber. The total color difference parameter (ΔE* was calculated according to the following formulation (3) (Chorobiński et al. 2019):

$$\Delta E^* = \sqrt{[(\Delta L^*)^2 + (\Delta a^*)^2 + (\Delta b^*)^2]} \quad (3)$$

Results and Discussion

Characterization of the copper slag (ŻŻL) Filler

The chemical composition analysis of the ŻŻL filler was based on the energy-dispersive X-ray spectroscopy technique (Figure 2). The obtained filler is a residue of the high-temperature copper production process. According to previous research the copper slag used in presented study mainly consists of SiO_2 (41.2%), Al_2O_3 (19.1%), CaO (13.1%), FeO and Fe_2O_3 (12.0%), MgO (4.9%), Cu (1.1%) (Hejna et al. 2018). The obtained EDS results confirm the presence of the mentioned chemical components, qualitatively, and quantitatively.

In Figure 3, FTIR spectra of neat PE and PE-ŻŻL composites are presented. Hardly any difference between spectra can be noted, which points to the lack of changes in the chemical structure of PE matrix and chemical interactions between phases. For all samples were noted signals at 2850 and 2915 cm^{-1}, attributed to the symmetric and asymmetric stretching vibrations of C-H bonds. Peaks related to their bending deformations were noted at 1455 cm^{-1}, while signals around 720 cm^{-1} were associated with the rocking vibrations of PE macromolecule. The presence of these signals is strictly related to the chemical structure of polyethylene (Figure 1).

Moreover, with the increasing content of the ŻŻL, the presence of signals between 800 and 1250 cm^{-1} can be noted. They may be attributed to the slight decomposition of the PE matrix during processing as a result of relatively high loading of very rigid filler, which generated high shear forces in the extruder barrel. As a result, partial oxidation may occur, which results in the generation of C-O bonds (Ołdak et al. 2005). Nevertheless, the lack of absorption bands related to the presence of carbonyl groups around 1740 cm^{-1} indicates that the degree of decomposition was very low (Gulmine et al. 2003).

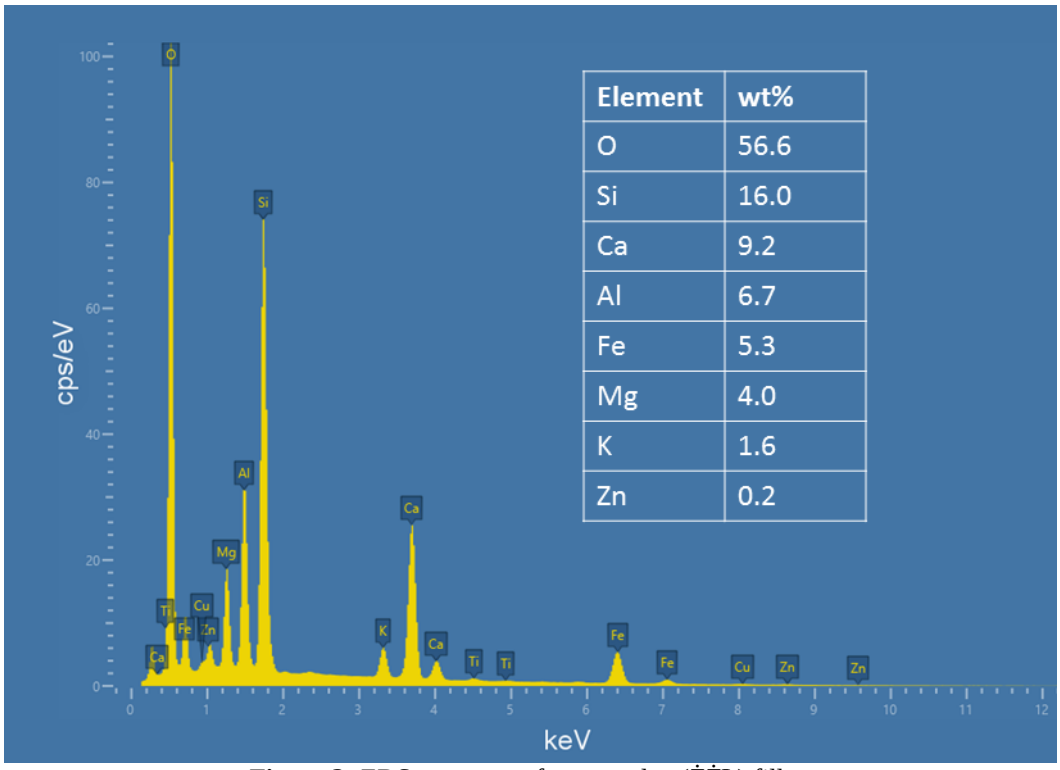

Figure 2: EDS spectrum of copper slag (ŻŻL) filler.

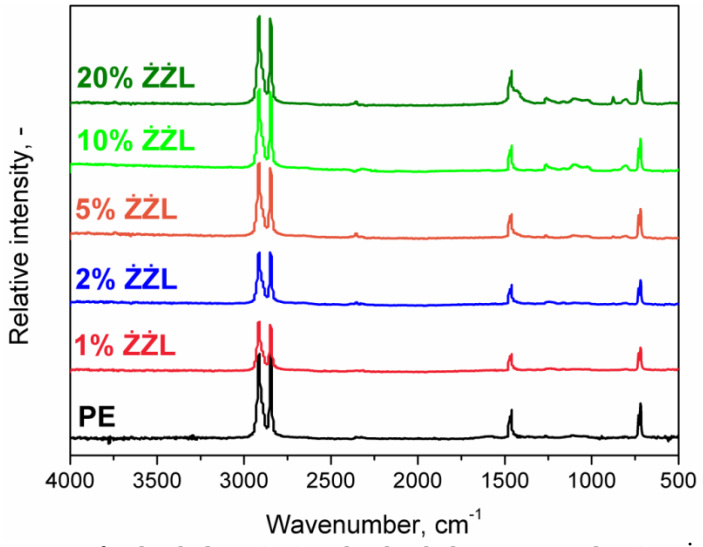

Figure 3: FTIR spectra of polyethylene (PE) and polyethylene-copper slag (PE-ŻŻL) composites.

The microstructure of PE-ŻŻL composites

Figure 4 shows microscopic images of the copper slag (ŻŻL) filler and surface of polyethylene (PE) and PE-ŻŻL composites. The filler has a small aspect ratio and the size of the sharply shaped particles do not exceed 250 μm. Analysis of the microscopic images revealed that the average particle size of the introduced ŻŻL filler could be assumed as ~130 μm. Homogeneous distribution of the filler is observed for all composite samples. However, single clusters of the filler can be distinguished, especially in the case of the lower ŻŻL content. Moreover, in Figure 4, there are also presented values of the average interparticle distance between ŻŻL particles (D) calculated by the following equation (4) (Hong et al. 2003):

$$D = r\left[\left(\frac{4\pi}{3\nu}\right)^{1/3} - 2\right] \qquad (4)$$

where: r = average radius of ŻŻL particle, μm; ν = volume fraction of ŻŻL.

In the case of the 10% ŻŻL sample, there was a change in color and loss of partial transparency of the material sample. During the shaping process, a polymer layer was formed on the surface of the material, thanks to which exposed inorganic filler particles are not observed. This significantly increases the resistance of composite materials to external conditions by limiting the potential of water absorption by the copper slag particles or the matrix-filler interface (Najafi et al. 2006).

Physico-mechanical properties of PE-ŻŻL composites

Incorporation of solid mineral particles into polyethylene matrix is associated with the increased density of composites considering significant differences in the densities of matrix and filler (0.954 and 3.040 g/cm^3, respectively for PE and ŻŻL). Such an effect was also noted for prepared composites. In Figure 5, there are presented measured values of their density together with theoretical values calculated by a simple rule of mixture (formula 1). These values were used to calculate the porosity of composites, which may significantly affect their performance (Sałasińska et al. 2016). Such an effect is mainly associated with the air inclusions due to the agglomeration of filler particles.

In Figure 6, there are presented results of tensile tests for polyethylene-copper slag (PE-ŻŻL) composites as a function of filler loading and applied strain rate during the test. The increase of the ŻŻL content resulted in a slight decrease of tensile strength from 23.33 to 20.48 MPa and from 27.87 to 23.07 MPa, respectively, for test speed of 5 and 50 mm/min. The reduction was also noted for the elongation at break; however, in this case, higher values were observed for lower test speed. The drop in the mechanical parameters is strictly associated with the increase of porosity, which results in the discontinuity of composites' structure.

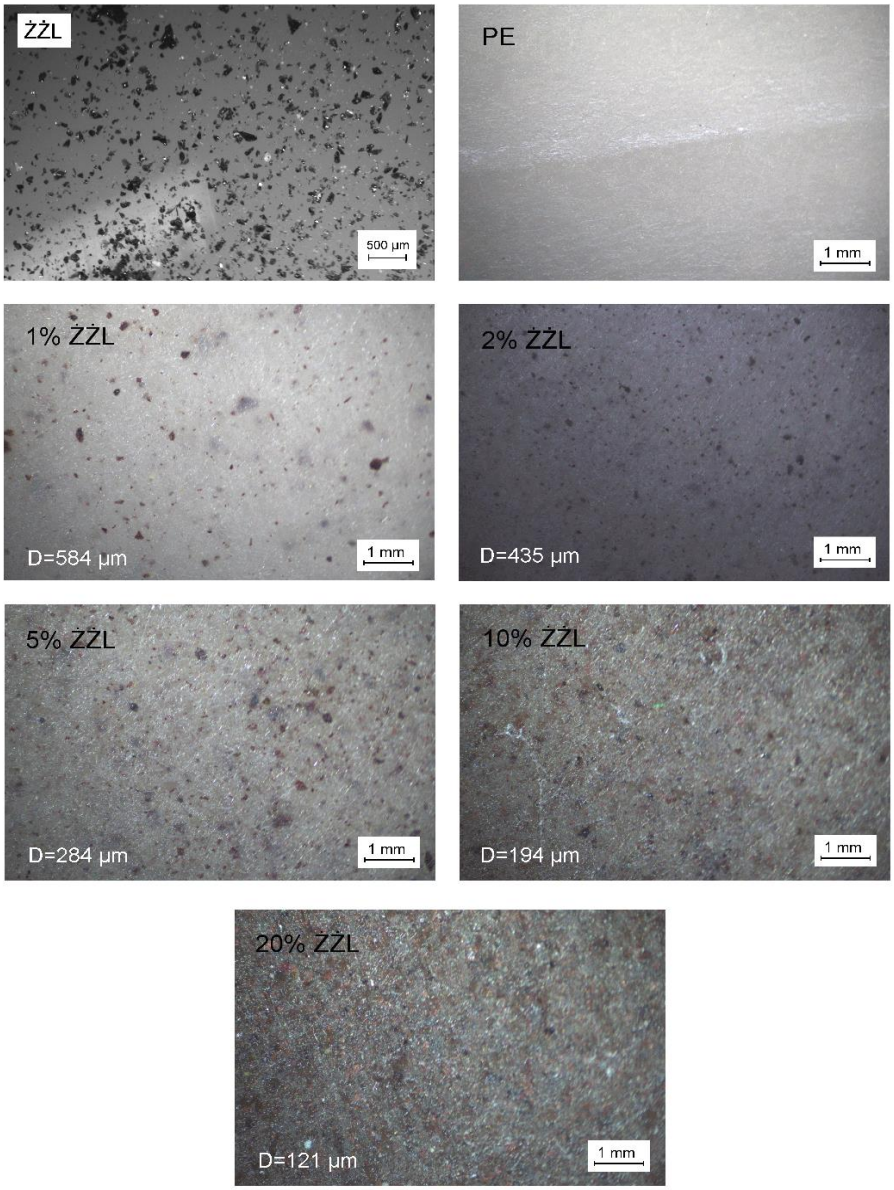

Figure 4: Microscope images of polyethylene (PE) and polyethylene-copper slag (PE-ŻŻL) composites surface obtained with reflecting optical microscope.

Higher values of tensile strength for higher strain rate during the tensile test are associated with the viscoelastic nature of polyethylene, especially the viscous component, whose behavior when strain is applied can be described by Newton's law (Brougham and Vaux and Routh 1855), expressed by the following formula (5):

$$\sigma = \eta\dot{\varepsilon} \quad (5)$$

where: σ = stress, η = viscosity, and ε = strain rate.

According to Newton's law, for viscoelastic materials, strength and elongation at break are strictly associated with the strain rate, which is related to the ability of macromolecular chains to achieve optimal alignment along the strain direction.

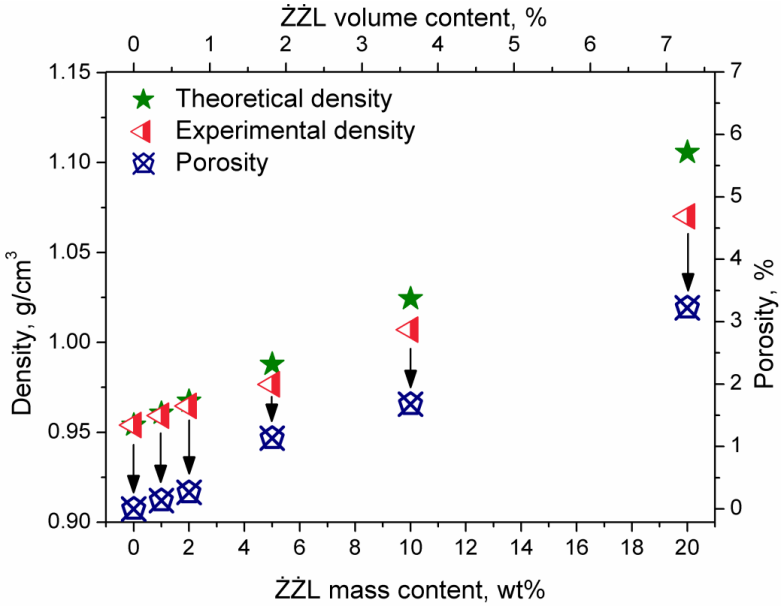

Figure 5: Structural properties of the polyethylene-copper slag (PE-ŻŻL) composites.

The results of tensile tests were also used to determine the values of composites' toughness by the integration of stress-strain curves. Figure 6c shows the schematic integration for the selected sample. Toughness represents the total amount of energy that can be absorbed or dispersed by the material. Ideally, tough material should be characterized by high values of tensile strength and elongation at break. For prepared composites, toughness is significantly dropping with the copper slag (ŻŻL) content, which is associated with the drop of elongation at break due to discontinuity of structure caused by the porosity.

Figure 6d presents the values of composites Young's modulus, which indicates that the stiffening of the structure was observed as a result of ŻŻL introduction. Such an effect of improved stiffness after incorporation of filler is rather typical for composite materials and was observed by other researchers (Bosenbecker et al. 2019, Kosciuszko et al. 2020, Oliwa et al. 2020).

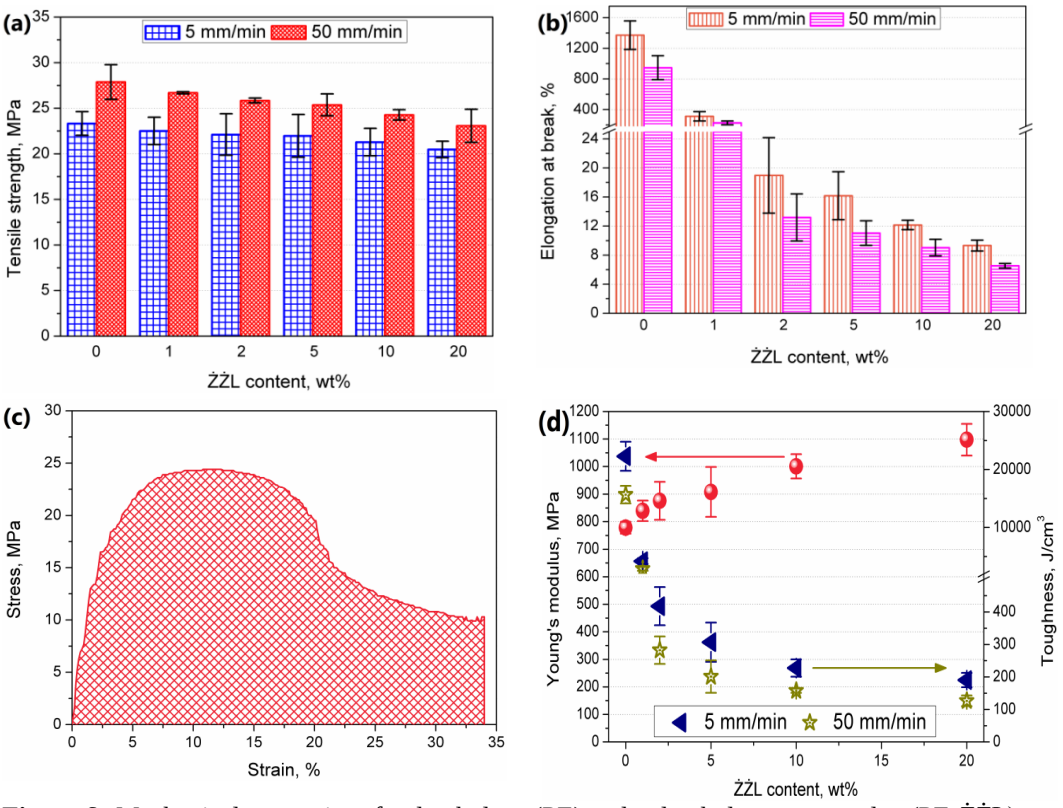

Figure 6: Mechanical properties of polyethylene (PE) and polyethylene-copper slag (PE-ŻŻL) composites: (a) tensile strength, (b) elongation at break, (c) schematic calculation of composites' toughness, (d) Young's modulus and toughness.

It can be seen that the tensile strength is decreasing almost proportionally to the ŻŻL content, hence also porosity of composite, while for elongation at the break, the effect of increasing filler loading is significantly higher. In order to evaluate the impact of composition and microstructure on the mechanical performance, we performed fitting of curves to model these relationships, as can be seen in Figure 7 for tensile strength. We have selected power functions because of their highest compatibility with obtained data.

It can be seen that for tensile strength, the exponent values are very close to 0, indicating that for the analyzed composites, strength was only slightly affected by porosity of structure. On the other hand, for elongation at break, values of exponents were -0.917 and -0.913, respectively, for test speeds of 5 and 50 mm/min. Such results indicate that discontinuity of structure has a significantly higher impact on the elongation at break than tensile strength.

For a more detailed analysis of the composites' structure and its impact on the mechanical performance, we performed the dynamic mechanical analysis. In our previous work (Mysiukiewicz et al. 2020), we presented a method of calculation of adhesion factor, based on the methodology proposed by Kubát et al. (1990), following the formula (6):

$$A = \left(\frac{1}{1-v_f}\right) \cdot \left(\frac{tan\delta_c}{tan\delta_m}\right) - 1 \qquad (6)$$

where: A = adhesion factor; ν = volume fraction of ŻŻL; $tan\ \delta_c$ and $tan\ \delta_m$ = values of loss tangent of composite and matrix.

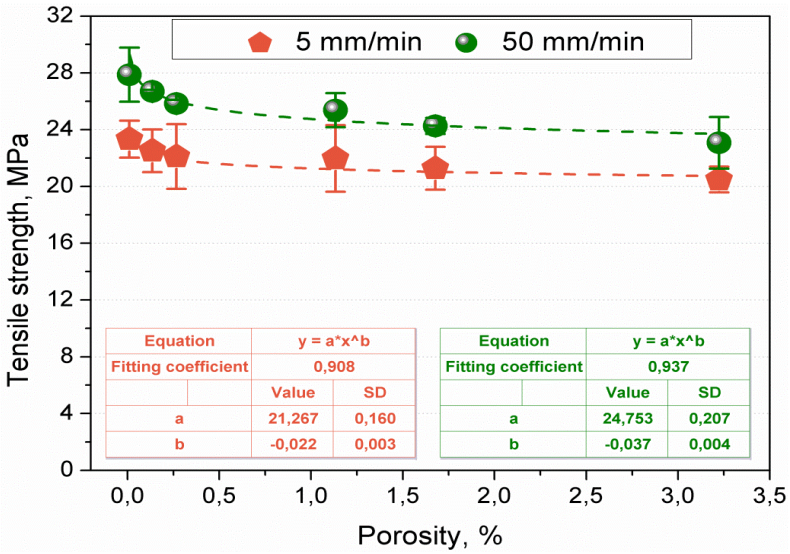

Figure 7: Dependency between tensile strength and porosity of polyethylene (PE) and polyethylene-copper slag (PE-ŻŻL) composites obtained for different strain rates.

The adhesion factor can be used to determine the quality of interfacial interactions between matrix and filler. Its lower values indicate enhanced adhesion. Negative values are due to the simplifications and assumptions made during calculations, which were described in our previous work (Mysiukiewicz et al. 2020). It can be seen that the adhesion factor is increasing with the ŻŻL content, which points to the reduced strength of interfacial interactions. Such an effect can be related to the lack of chemical bonding between phases, as suggested by FTIR spectra, as well as the porosity of structure, which generates discontinuity of composites' structure. In Figure 8, we presented the dependence of the adhesion factor and porosity. It can be seen that these parameters are almost proportionally related to each other, indicating that in the presented case, the porosity of structure is crucial for the interfacial adhesion. Presented results confirm the reduction of mechanical parameters with the increasing filler loading.

Moreover, the results of the DMA analysis were used to calculate the brittleness of the material, according to the formula (7) presented by Brostow et al. (2006):

$$B = \frac{1}{(\varepsilon_b \cdot E')} \quad (7)$$

where: B = brittleness, 10^{10} %·Pa; ε_b = elongation at break, %; E' = storage modulus at 25 °C, MPa.

The idea of brittleness is quite similar to the toughness, indicating that material with low brittleness should be able to withstand possibly high stress at the possibly widest range of strains. Therefore, brittleness stands as the antagonist of toughness. In their work, Brostow et al. (2006) related these two parameters by the rational function, however, we prefer the use of power function, which was also described in our previous work (Galeja et al. 2020), where we connected these parameters by the following equation (8):

$$\tau = aB^c \quad (8)$$

where: τ = toughness, J/cm^3; B = brittleness, 10^{10} %·Pa.

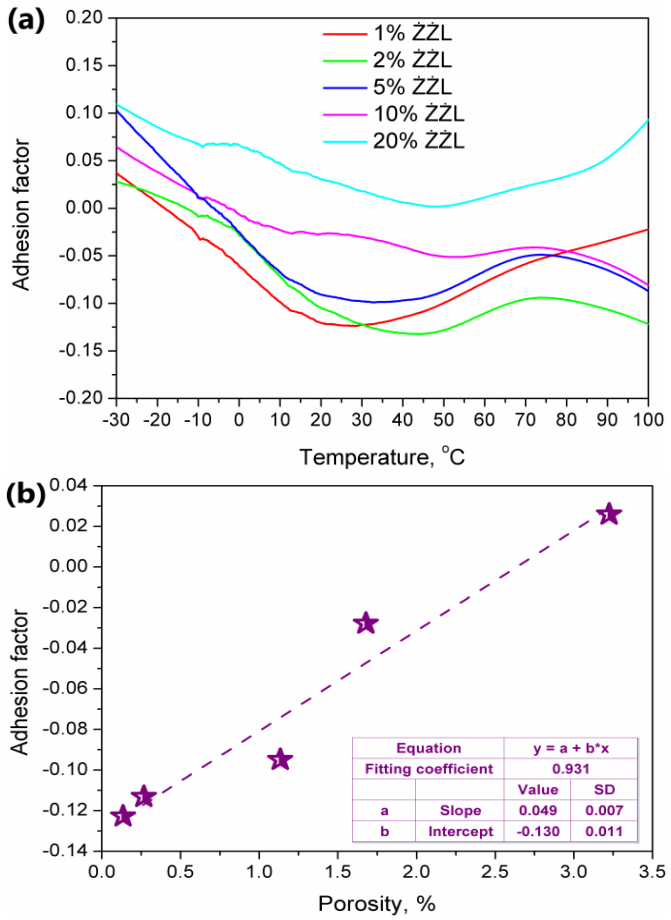

Figure 8: Adhesion factor as a function of temperature (a) and porosity (b) determined by DMA analysis.

Figure 9 shows the plot, where the relationship between these two parameters was presented. For data presented by Brostow et al. (2006), values of *a* and *c* were 178.380 and -0.984, respectively. Nevertheless, it can be seen that data points for PE-ŻŻL composites lie below the literature curve. Such an effect is associated with the fact that they investigated the performance of homogenous materials, such as polymers or metals. Therefore, no influence of interfacial adhesion was considered. For PE-ŻŻL composites, values of *a* were 104.180 and 69.414, while values of exponent *c* were very similar to literature data and equaled -0.976 and -0.984, respectively, for tensile test speed of 5 and 50 mm/min. It indicates that the relationship between brittleness and toughness is very similar. However, due to the additional effects of interfacial interactions, which are usually weaker than the cohesion of polymer, values of mechanical parameters were lower than for homogenous materials.

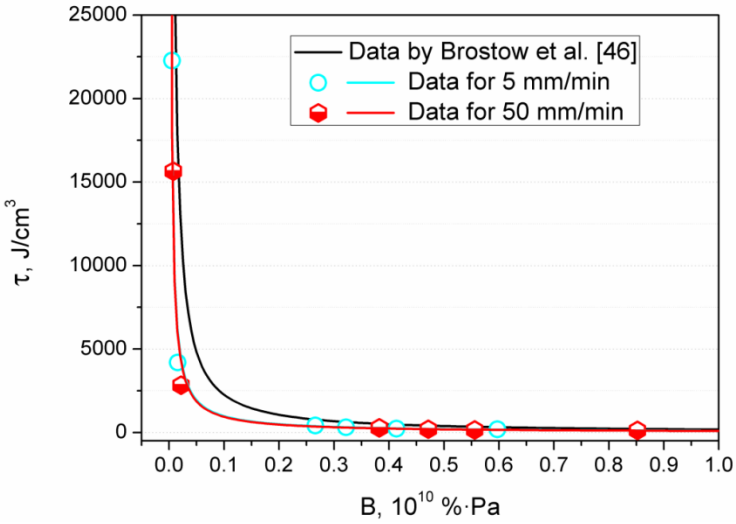

Figure 9: Toughness vs. brittleness of polyethylene-copper slag (PE-ŻŻL) composites.

The color change of polymers caused by the addition of a filler can significantly increase its attractiveness and commercialization possibilities. The most used color analysis is the description of the color change in the CIELab space. It can be used for qualitative analysis of color change as well as for the indirect assessment of degradation effects occurring as a result of processing processes and aging (Colin and Verdu 2006, Moraczewski et al. 2019). Figure 10 summarizes the changes in parameters L*, a*, b*, and the total color difference ΔE of the PE composites in the ŻŻL function filler content. The color parameters registered for the filler are marked with a red line. The addition of ŻŻL caused a significant change in color. The value of the parameter describing luminescence was reduced from 85 to about 30. In the case of composites containing 10 and 20 wt% of ŻŻL, the value of L was comparable to the parameter measured for the filler itself. The addition of filler caused a significant change in the values of parameters a and b, the highest values were recorded for composites containing 2 and 5 wt%. Afterward, the values of a and b decreased. In the case of L and b parameters, the values recorded for composites with the highest degree of filling are similar to the characteristics made for the filler. In the case of composite samples containing 10 and 20 wt% ŻŻL, the samples became entirely opaque and brown. When 10 wt% ŻŻL was used, a saturation of the filler relative to the color change was achieved. Further increasing the content of the waste filler did not cause significant changes in the total color difference parameter. In the case of all composite samples, the ΔE changes are greater than 5, which concerning the PN-EN ISO 2813: 2001 standard, indicates large color variations (Bociaga and Trzaskalska 2016). As the results of the color analysis suggest, the appearance of the ŻŻL-filled polyethylene changes with the addition of filler. Therefore, by adjusting the copper slag content, a wide variety of colors tuned for a specific application can be obtained.

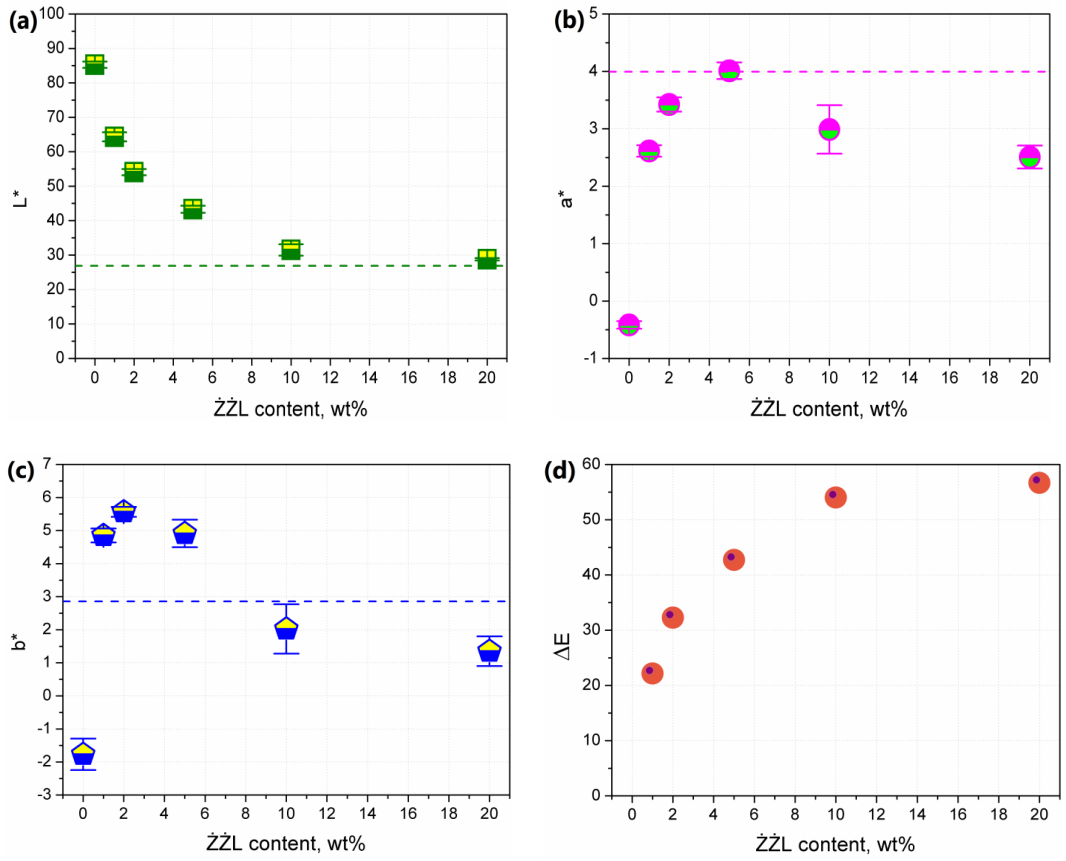

Figure 10: CIELab parameters: (a) lightness, (b) a*, (c) b*, and (d) total color change of polyethylene (PE) and polyethylene-copper slag (PE-ŻŻL) samples.

Conclusions

The presented research paper was aimed at investigating the impact of copper slag filler on the structure and mechanical performance of PE-ŻŻL composites. Microscopic analysis revealed that applied filler was adequately dispersed in the thermoplastic polyethylene matrix. Nevertheless, during sample preparation, portions of air were introduced into the composites' structure, resulting in its porosity. Such an effect, together with the lack of chemical bonding between phases, as indicated by FTIR spectroscopic analysis, resulted in the slight deterioration of the mechanical performance. Nevertheless, up to the 5 wt% content of the ŻŻL filler, only a 5% drop of tensile strength was observed, with the simultaneous 16% rise of modulus. Higher loadings resulted in the rise of the adhesion factor, indicating weakened interfacial interactions, hence lower values of the mechanical properties. Moreover, spectroscopic analysis of PE-ŻŻL composites indicated that analyzed filler might be applied as a coloring agent, and the appearance of composites may be engineered by adjustment of filler loading.

Conflict of interest

The authors confirm that this work has no conflicts of interest.

References

Al-Jabri KS, Al-Saidy AH and Taha R 2011 Effect of copper slag as a fine aggregate on the properties of cement mortars and concrete. *Constr. Build. Mater.* 25: 933–938.

Andrzejewski J, Misra M and Mohanty AK 2018 Polycarbonate biocomposites reinforced with a hybrid filler system of recycled carbon fiber and biocarbon: Preparation and thermomechanical characterization. *J. Appl. Polym. Sci.* 135: 46449.

Arora G and Pathak H 2020 Experimental and numerical approach to study mechanical and fracture properties of high-density polyethylene carbon nanotubes composite. *Mater. Today Commun.* 22: 100829.

Bajwa SG, Bajwa DS and Anthony AS 2009 Effect of laboratory aging on the physical and mechanical properties of wood-polymer composites. *J. Thermoplast. Compos. Mater.* 22: 227–243.

Barczewski M, Sałasińska K, Kloziński A, Skórczewska K, Szulc J and Piasecki A 2019 Application of the Basalt Powder as a filler for polypropylene composites with improved thermo-mechanical stability and reduced flammability. *Polym. Eng. Sci.* 59: 71–79.

Bhagavatheswaran ES, Das A, Rastin H, Saeidi H, Jafari SH, Vahabi H, Najafi F, Khonakdar HA, Formela K, Jouyandeh M, Zarrintaj P and Saeb MR 2019 The taste of waste: the edge of eggshell over calcium carbonate in acrylonitrile butadiene rubber. *J. Polym. Environ.* 27: 2478–2489.

Bociaga E and Trzaskalska M 2016 Influence of polymer processing parameters and coloring agents on gloss and color of acrylonitrile-butadiene-styrene terpolymer moldings. *Polimery* 61: 544–550.

Bosenbecker MW, Cholant GM, da Silva GEH, Paniz OG, Carreño NLV, Marini J and de Oliveira AD 2019 Mechanical characterization of HDPE reinforced with cellulose from rice husk biomass. *Polímeros* 29(4). doi:10.1590/0104-1428.04819.

Brostow W, Hagg Lobland HE and Narkis M 2006 Sliding wear, viscoelasticity, and brittleness of polymers. *J. Mater. Res.* 21: 2422–2428.

Brougham H, Brougham HB and Routh EJ 1855 Analytical view of Sir Isaac Newton's Principia, Palala Press, London.

Burzynski M, Paszkiewicz S, Piesowicz E, Irska I, Dydek K, Boczkowska A, Wysocki S and Sieminski J 2020 Comparison study of the influence of carbon and halloysite nanotubes on the preparation and rheological behavior of linear low density polyethylene. *Polimery* 65: 95–98.

Chorobiński M, Skowronski L and Bielinski M 2019 Methodology for determining selected characteristics of polyethylene dyeing using CIELab system. *Polimery* 64: 690–696.

Colin X and Verdu J 2006 Polymer degradation during processing. *Comptes Rendus Chim.* 9: 1380–1395.

Czarnecka-Komorowska D and Wiszumirska K 2020 Zrównoważone projektowanie opakowań z tworzyw sztucznych w gospodarce cyrkularnej. *Polimer*y 65: 8–17.

Członka S, Strąkowska A and Kairytė A 2020 Effect of walnut shells and silanized walnut shells on the mechanical and thermal properties of rigid polyurethane foams. *Polym. Test.* 87: 106534.

Erdenebold U, Choi HM and Wang JP 2018 Recovery of pig iron from copper smelting slag by reduction smelting. *Arch. Metall. Mater.* 63: 1793–1798.

Fortune Business Insights 2019 Polyethylene (PE) market size, share and industry analysis, by type (HDPE, LDPE, LLDPE), by end user (packing, automotive, infrastructure and construction, consumer, goods/lifestyle healthcare and pharmaceutical, electrical and electronics, agriculture, others), October 2019. Available at: https://www.fortunebusinessinsights.com/industry-reports/polyethylene-pe-market-101584.

Friedrich D and Luible A 2016 Investigations on ageing of wood-plastic composites for outdoor applications: A meta-analysis using empiric data derived from diverse weathering trials. *Constr. Build. Mater.* 124: 1142–1152.

Galeja M, Hejna A, Kosmela P and Kulawik A 2020 Static and dynamic mechanical properties of 3D printed ABS as a function of raster angle. *Materials* 13: 297.

Gnatowski A, Kazik E and Palutkiewicz P 2018 Investigation of properties of molded parts made of polyethylene with addition of ash from bituminous coal. *Compos. Theory Pract.* 18: 127–132.

Gorai B, Jana, RK and Premchand 2003 Characteristics and utilisation of copper slag–a review. *Resour. Conserv. Recycl.* 39: 299–313.

Gulmine JV, Janissek PR, Heise HM and Akcelrud L 2003 Degradation profile of polyethylene after artificial accelerated weathering. *Polym. Degrad. Stab.* 79: 385–397.

Gunjal J, Aggarwal P and Chauhan S 2020 Changes in colour and mechanical properties of wood polypropylene composites on natural weathering. *Maderas. Cienc. y Tecnol*. In Press. doi:10.4067/S0718-221X2020005000307.

He X, Cai Y, Wang Q, Qi X, Guo R, Tang Y and Liu B 2012 Improvement of mechanical properties and ultraviolet resistance of polyethylene pipe materials using high density polyethylene matrix grafted carbon black. *J. Macromol. Sci. Part B Phys.* 51: 298–312.

Hejna A, Piszcz-Karaś K, Filipowicz N, Cieśliński H, Namieśnik J, Marć M, Klein M and Formela K 2018 Structure and performance properties of environmentally-friendly biocomposites based on poly(ε-caprolactone) modified with copper slag and shale drill cuttings wastes. *Sci. Total Environ.* 640–641: 1320–1331.

Hong JI, Schadler LS, Siegel RW and Mårtensson E 2003 Rescaled electrical properties of ZnO/low density polyethylene nanocomposites. *Appl. Phys. Lett.* 82: 1956–1958.

International Commission on Illumination 1978 Recommendations on uniform color spaces, color-difference equations, psychometric color terms, Bureau central de la CIE, Paris.

Kairytė A, Kremensas A, Vaitkus S, Członka S and Strąkowska A 2020 Fire suppression and thermal behavior of biobased rigid polyurethane foam filled with biomass incineration waste ash. *Polymers* 12: 683.

Kalaprasad G, Joseph K and Thomas S 1997 Influence of short glass fiber addition on the mechanical properties of sisal reinforced low density polyethylene composites. *J. Compos. Mater.* 31: 509–527.

Kasirajan S and Ngouajio M 2012 Polyethylene and biodegradable mulches for agricultural applications: a review. *Agron. Sustain. Dev.* 32: 501–529.

Kosciuszko A, Czyżewski P, Wajer Ł, Osciak A and Bielinski M 2020 Properties of polypropylene composites filled with microsilica waste. *Polimery* 65: 99–104.

Kubát J, Rigdahl M and Welander M 1990 Characterization of interfacial interactions in high density polyethylene filled with glass spheres using dynamic-mechanical analysis. *J. Appl. Polym. Sci.* 39: 1527–1539.

Li B and Li R 2016 Preparation and property of ultrahigh molecular weight polyethylene/halloysite nanotube fiber. *Fibers Polym.* 17: 1043–1047.

Luo W, Cheng C, Zhou S, Zou H and Liang M 2015 Thermal, electrical and rheological behavior of high-density polyethylene/graphite composites. *Iran. Polym. J.* 24: 573–581.

Moraczewski K, Stepczyńska M, Malinowski R, Karasiewicz T, Jagodziński B and Rytlewski P 2019 The effect of accelerated aging on polylactide containing plant extracts. *Polymers* 11: 575.

Mugford C, Gibbs JL and Boylstein R 2017 Elemental properties of copper slag and measured airborne exposures at a copper

slag processing facility. *J. Occup. Environ. Hyg*. 14: 120–129.

Mysiukiewicz O, Kosmela P, Barczewski M and Hejna A 2020 Mechanical, thermal and rheological properties of polyethylene-based composites filled with micrometric aluminum powder. *Materials* 13: 1242.

Najafi SK, Tajvidi M and Chaharmahli M 2006 Long-term water uptake behavior of lignocellulosic-high density polyethylene composites. *J. Appl. Polym. Sci.* 102: 3907–3911.

Niemczyk A, Adamczyk-Tomiak K, Dziubek K, Czaja K, Rabiej S, Szatanik R and Dutkiewicz M 2019 Study of polyethylene nanocomposites with polyhedral oligomeric silsesquioxane nanofillers-from structural characteristics to mechanical properties and processability. *Polym. Compos.* 40: 350–364.

Niemczyk A, Dziubek K, Sacher-Majewska B, Czaja K, Dutkiewicz M and Marciniec B 2016 Study of thermal properties of polyethylene and polypropylene nanocomposites with long alkyl chain-substituted POSS fillers. *J. Therm. Anal. Calorim*. 125: 1287–1299.

Oliwa R, Bulanda K, Oleksy M, Ostynska P, Budzik G, Plocinska M and Krauze S 2020 Fire resistance and mechanical properties of powder-epoxy composites reinforced with recycled glass fiber laminate. *Polimery* 65: 280–288.

Ołdak D, Kaczmarek H, Buffeteau T and Sourisseau C 2005 Photo- and bio-degradation processes in polyethylene, cellulose and their blends studied by ATR-FTIR and Raman spectroscopies. *J. Mater. Sci*. 40: 4189–4198.

Peterlin A 1971 Molecular model of drawing polyethylene and polypropylene. *J. Mater. Sci*. 6: 490–508.

Rudawska A, Jakubowska P and Klozinski A 2017 Surface free energy of composite materials with high calcium carbonate filler content. *Polimery* 62: 434–440.

Ryszkowska J and Sałasińska K 2010 Kompozyty z folii oksybiodegradowalnej z recyklingu napełniane drewnem. *Polimery* 55: 740–747.

Sałasińska K, Polka M, Gloc M and Ryszkowska J 2016 Natural fiber composites: the effect of the kind and content of filler on the dimensional and fire stability of polyolefin-based composites. *Polimery* 61: 255–265.

Sałasińska K and Ryszkowska J 2013 Dimensional stability, physical, mechanical and thermal properties of high density polyethylene with peanut hulls composites. *Polimery* 58: 461–466.

Sałasińska K, Borucka M, Celiński M, Gajek A, Zatorski W, Mizera K, Leszczyńska M and Ryszkowska J 2018 Thermal stability, fire behavior, and fumes emission of polyethylene nanocomposites with halogen-free fire retardants. *Adv. Polym. Technol.* 37(7): 2394–2410.

Shi C, Meyer C and Behnood A 2008 Utilization of copper slag in cement and concrete. *Resour. Conserv. Recycl.* 52: 1115–1120.